Computational and Theoretical Chemistry 1068 (2015) 134–141

Contents lists available at ScienceDirect

Computational and Theoretical Chemistry

journal homepage: www.elsevier.com/locate/comptc

Cross-cluster transition-metal bonding in oblato-nido dimetallaboranes unveiled by topological analysis

Benoît Boucher [a,b], Jean-François Halet [a], Miroslav Kohout [b,*]

[a] *Institut des Sciences Chimiques de Rennes, UMR 6226 CNRS-Ecole Nationale Supérieure de Chimie de Rennes-Université de Rennes 1, Avenue du Général Leclerc, 35042 Rennes, France*

[b] *Max-Planck-Institut für Chemische Physik fester Stoffe, Nöthnitzer Strasse 40, 01187 Dresden, Germany*

ARTICLE INFO

Article history:
Received 5 May 2015
Received in revised form 25 June 2015
Accepted 26 June 2015
Available online 6 July 2015

Keywords:
Metal–metal bond
Atoms in molecules
Delocalization index
Electron localizability indicator

ABSTRACT

The bonding situation for the oblato-nido dimetallaboranes $(CpV)_2B_5H_{11}$ and $(Cp^{*}T)_2B_5H_{5+x}$, where T = Ta, Cr, Mo, W, Re and $Cp^{*} = C_5Me_5$, was analyzed using the corresponding model series with Cp^{*} replaced by the cyclopentadienyl C_5H_5. The application of different bonding indicators revealed that both through-space and through-bond (via boron atoms of the ring) interactions account for a substantial metal–metal bond.

1. Introduction

There are today over hundred molecular dimetallaboranes, which have been synthesized and characterized with nearly all the transition metals (T), both early and late metals (see for example Fehlner et al. [1–3]). They constitute a class of compounds which has revealed numerous possibilities for the way metal and borane fragments interact to generate novel structures, demonstrating the important role for the transition metal in the structural arrangements which are observed. Among these compounds the molecules $(CpV)_2B_5H_{11}$ [4], $(Cp^{*}Cr)_2B_5H_9$ [5], $(Cp^{*}Mo)_2B_5H_9$ [6], $(Cp^{*}Ta)_2B_5H_{11}$ [6], $(Cp^{*}W)_2B_5H_9$ [3], and $(Cp^{*}Re)_2B_5H_2Cl_5$ [7], whereby $Cp^{*} = C_5Me_5$, constitute examples of early transition-metal dimetallaboranes which all adopt the same open and flattened hexagonal bipyramidal *nido* geometry and possess the electron count of 12 cluster valence electrons. Their structural peculiarities are the oblate (i. e., flattened) shape (these compounds are termed as oblato-nido species) [8] and the fact that the metal atoms occupy opposite vertexes in such a way that the $T–T$ distance is consistent with possible existence of a cross-cluster bonding interaction. Indeed, short $T–T$ distances have been measured experimentally [3–7]. Such structures are apparently highly hypoelectronic and do not obey the Wade–Mingos rules [9–11] as generally do boranes, carboranes and late-transition metallaboranes. Density functional theory (DFT) calculations have been able to sort out this apparent systematic rule deviation [7], but the proximity of the two metal atoms on opposite sides in the flattened direction allows some speculation about the nature of $T–T$ interaction. This has been tackled several times in the literature using MO analysis [1,2,7,8,12–20]. However, whereas the conclusions seem to fully converge with some studies evidencing a single $T–T$ bond [7], some others suggest a formal internal $T–T$ double bond [8].

In the following, the through-space $T–T$ interaction in the $CpT_2B_5H_{5+x}$ model series, with the number of bridging (H_b) atoms $x = 6$ for V, Ta, $x = 4$ for Cr, Mo, W, and $x = 2$ for Re, respectively, is analyzed. The investigation was performed using the electron density and its derivatives within the framework of the quantum theory of atoms in molecules [21] (QTAIM), as well as utilizing several bonding indicators like the delocalization indices [22,23] (DI), the Fermi orbitals (FO) from the domain-averaged Fermi-hole analysis [24–26] (DAFH), the covalent bond order from the evaluation of localized natural orbitals (LNO) [27], and the electron localizability indicator ELI-D [28,29].

2. Theory section

2.1. Electronic structure calculations

The calculations were performed with the Gaussian09 program [30] at the density-functional level of theory (DFT). The

---

* Corresponding author.
E-mail address: kohout@cpfs.mpg.de (M. Kohout).

http://dx.doi.org/10.1016/j.comptc.2015.06.029
2210-271X/© 2015 Elsevier B.V. All rights reserved.

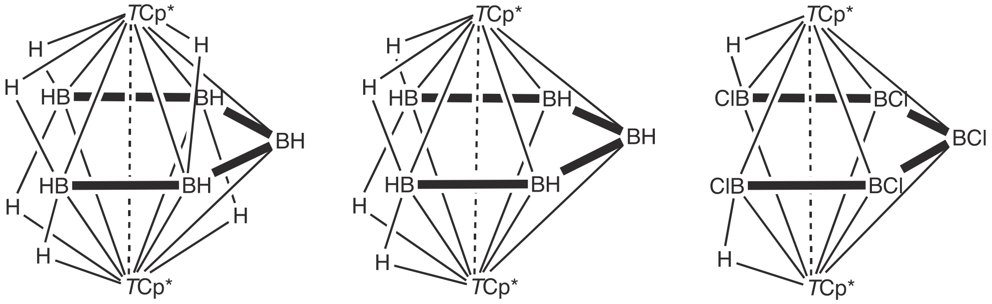

T = V, Ta *T* = Cr, Mo, W *T* = Re

Fig. 1. The oblato-nido species.

computational demand for the oblato-nido species, cf. Fig. 1, was reduced replacing $Cp^* = C_5Me_5$ by $Cp = C_5H_5$ and Cl by H. This substitution is not expected to have significant influence on the analysis. The atoms H, B, C and O were described by the 6-31G** basis sets and the *T* atoms by the corresponding LANL2DZ basis sets utilizing effective core potentials. For the DFT calculations the BVP86 functional was used [31–33]. The structure of the examined model systems was optimized and the harmonic vibrational frequencies were computed to check the stationarity of the optimized geometries.

2.2. Methods

The calculation of the bonding indicators and the topological analysis was performed with the DGrid-4.6 program [34]. The electron density, the ELI-D, and the Fermi orbitals were computed on equidistant grids using a 0.1 bohr mesh size.

Following the QTAIM approach the electron density was searched for critical points (points of zero density gradient in case of Gaussian basis) and several properties were evaluated at the saddle points (so-called bond-critical points, *bcp*). For each *bcp* the bond path, representing the bonding interaction, was computed. The density basins (spatial regions enclosed by density-gradient zero-flux surfaces) were determined and the electronic population within evaluated, leading to the effective charges of the atomic regions. Additionally, the overlap integrals over the QTAIM basins were computed. Those were utilized to compute the delocalization indices (DI), connected with the bond order, as well as the Fermi orbitals (FO) and the localized natural orbitals (LNO).

3. Results and discussions

3.1. Structure optimization

The experimental interatomic distances between the two transition metals, together with the (averaged) distances from the *T* to the carbon and boron, respectively, in the oblato-nido species under consideration are compiled in Table 1.

Table 1
Interatomic distances from experiment (Å).

Compound	*T*–*T*	*T*–C[a]	*T*–B[a]
$(CpV)_2B_5H_{11}$	2.7604(10) [4]	2.247	2.217
$(Cp^*Cr)_2B_5H_9$	2.6246(9) [6]	2.198	2.147
$(Cp^*Mo)_2B_5H_9$	2.8085(6) [6]	2.328	2.248
$(Cp^*Ta)_2B_5H_{11}$	2.9261(4) [5]	2.384	2.326
$(Cp^*W)_2B_5H_9$	2.8170(8) [3]	2.326	2.239
$(Cp^*Re)_2B_5H_2Cl_5$	2.7641(3) [7]	2.292	2.201

[a] Averaged.

The geometry optimization of the corresponding model systems results in *T*–*T* distances deviating from the experimental ones within few pm only, cf. the data reported in Table 2 (see Supplementary data for the optimized model structures). In case of $(CpRe)_2B_5H_7$ the *trans* configuration of the two H_b atoms is energetically more favorable than the *cis* configuration as proposed earlier by others [7].

3.2. Bond paths

The evaluation of the critical points of the electron density distribution ρ followed by the search for the bond paths, i.e., field lines of $\nabla\rho$ connecting bond-critical points (saddle points) with attractors (ρ maxima) yields so-called molecular graph [21]. For each model system the corresponding molecular graph, cf. Fig. 2 closely resembles the classical chemical structure diagrams. The metal atoms are linked by a bond path to each carbon of the close Cp ligand. In case of the bridging hydrogens the corresponding paths are strongly curved, whereby the metal-boron path is not present, in contrast to Fig. 1 where the closest interatomic contacts are just schematically depicted.

The presence of *T*–*T* bonding interaction, as suggested by the short interatomic distance, was clearly confirmed by the existence of the bond-critical point and the corresponding bond path connecting the two metals. The *T*–*T* bond path was found for all the examined model systems. The density Laplacian at the *bcp* is positive in all cases, cf. Table 3, thus showing a charge depletion which would mark a “closed-shell” interaction. However, this is a situation not untypical for the *d*-metals [35,36]. Because of the relatively high electron density at the *bcp* (higher than twice the density of overlapping atoms) as well as the negative (though small) value of the energy density *H* (as indicated by the bond degree H/ρ [37]) the *T*–*T* interaction has a covalent character. Only for the Cr complex the $|V|/G$ ratio is close to 1, showing that the potential energy does not unfold the appropriate stabilizing influence on the Cr–Cr bond. Besides the V complex all the other systems yield a $|V|/G$ ratio close to 2, from where the density Laplacian at the *bcp* would revert from depletion to charge

Table 2
Optimized interatomic distances (Å).

Compound	*T*–*T*	*T*–C[a]	*T*–B[a]
$(CpV)_2B_5H_{11}$	2.691	2.281	2.221
$(CpCr)_2B_5H_9$	2.595	2.206	2.155
$(CpMo)_2B_5H_9$	2.828	2.364	2.266
$(CpTa)_2B_5H_{11}$	2.938	2.423	2.338
$(CpW)_2B_5H_9$	2.831	2.356	2.264
$(CpRe)_2B_5H_7$	2.745	2.315	2.201

[a] Averaged.